

We are IntechOpen, the world's leading publisher of Open Access books Built by scientists, for scientists

6,900

Open access books available

185,000

International authors and editors

200M

Downloads

Our authors are among the

154

Countries delivered to

TOP 1%

most cited scientists

12.2%

Contributors from top 500 universities



WEB OF SCIENCE™

Selection of our books indexed in the Book Citation Index
in Web of Science™ Core Collection (BKCI)

Interested in publishing with us?
Contact book.department@intechopen.com

Numbers displayed above are based on latest data collected.
For more information visit www.intechopen.com



Antisymmetrized Molecular Dynamics and Nuclear Structure

Gaotsiwe J. Rampho and Sofianos A. Sofianos
*Department of Physics, University of South Africa
South Africa*

1. Introduction

One of the aims of nuclear physics studies is to establish a complete theoretical description of the structure of nuclear systems. The correct theoretical description of nuclear structure is expected to help explain and accurately predict different properties of and process in nuclei (Donnelly & Raskin, 1986). Fundamental to a complete description of nuclear structure are the wave function describing nuclear systems, the Hamiltonian describing interactions in the nucleus and electromagnetic form factors describing charge and currents distributions in the nucleus. None of these components is completely understood and, therefore, none can be completely determined for a given nuclear system, yet. As a result, theoretical models of these components, based on different approximations that are guided by experimental observations, are usually employed in the description of nuclear systems. The quality of such models is often judged by their ability to explain existing experimental observations. Parallel to the theoretical developments, the developments in experimental technologies has led not only to the availability of more precise experimental data, but also to data in kinematical regions previously not accessible. The availability of precise experimental data in a wide kinematical region allow for more accurate quantitative testing and, therefore, development of realistic theoretical models that, in turn, generate more accurate predictions of experimental outcomes (Golak et al., 2005).

Besides the understanding of static and dynamical properties of nuclear matter, studies in nuclear physics are aimed at constructing a comprehensive description of properties of nucleon-nucleon interactions. Few-nucleon systems provide unique favourable environment for such investigations (Rampho, 2010). In theoretical investigations, the interaction models in few-nucleon systems can be treated realistically and the resulting dynamical equations can be solved directly. The formulation and solution of dynamical equations for many-body systems is, on the other hand, quite challenging. Progress towards a better understanding of the nuclear force has been made over the years. Based on the accumulated experimental nucleon-nucleon scattering data different phenomenological nucleon-nucleon interaction models have been suggested. The models are constructed by fitting the models to existing nucleon-nucleon scattering data as well as some properties of the ^2H nucleus (Cottingham et al., 1973; Lagaris & Pandharipande, 1981; Machleidt et al., 1987; Nagels et al., 1978; Wiringa et al., 1984). These interaction models are known as modern or realistic nucleon-nucleon potentials and are able to explain most of the static properties of light nuclei. Since the exact form of the short-range behavior of the nucleon-nucleon interaction is not completely determined, yet, the short-range part of many of these potential models is

often musked by introducing short-distance cut-off factors. Knowledge of the short-range behavior of the nucleon-nucleon force may reveal some information about the limits and boundaries between hadronic degrees of freedom and quark degrees of freedom. The suggestion that the short-range behavior of the strong nuclear interaction could manifest itself through short-range nucleon-nucleon correlations and momentum distributions in a nucleus (Schroeder et al., 1979) refocused the need for a better understanding of, and therefore more intensive investigations into, these concepts. Hence, there are continued experimental (Egiyan et al., 2007; 2006; Jones et al., 2000; Ulmer et al., 2002) and theoretical (Alvioli et al., 2008; Frankfurt et al., 1993; Piasetzky et al., 2006) investigations of these concepts.

Over the years a variety of methods have been developed and refined in the study of properties of nuclei. Very accurate wave functions for bound and scattering states in few-nucleon systems can now be constructed using realistic Hamiltonian for the systems. A demonstration of the level of accuracy that can now be achieved in describing ground state properties of the four-nucleon system using seven different state-of-the-art methods is given in reference (Kamada et al., 2001). The use of some of these methods in the study of properties of few-nucleon systems is shown in references (Carlson & Schiavilla, 1998; Golak et al., 2005). The application of these methods to systems consisting of more than four particles is still a challenge. For investigations of light to medium nuclei microscopic models have been employed in the study of static and dynamical properties of nuclei (Aichelin, 1991; Boffi et al., 1968; Kanada-En'yo et al., 2003; Neff et al., 2005; Ono & Horiuchi, 2004). These methods are continuously developing. Following the Time-Dependent Cluster Model (Caurier et al., 1982), microscopic simulation models were developed (Feldmeier, 1990; Horiuchi, 1991) for the study of fermionic systems. These models combine Fermi-Dirac statistics with elementary quantum mechanics to treat the motion of particles in a system (Feldmeier, 1990). However, the models are not fully quantum mechanical and do not assume a shell structure for the system. In this work the antisymmetrized molecular dynamics (AMD) approach is employed. The AMD total wave function is constructed as Slater determinant of single particle shifted Gaussian wave functions. The shift parameters of the Gaussian functions are complex variational parameters which are treated as generalised coordinates of the system. The width parameters are taken as free real parameters and are chosen to be the same for all the Gaussian. The equations of motion for the variational parameters are determined from the time-dependent variational principle. The equations are then solved by using the frictional cooling technique (Ono et al., 1992) to determine the variational parameters.

In the past, the AMD approach was employed in the study of dynamics of heavy-ion collisions (Ono et al., 1992) and elastic proton-nucleus scattering (Engel et al., 1995; Tanaka et al., 1995). Clustering in nuclei as well as angular distributions of scattered protons in proton-nucleus scattering can be well explained with the AMD model (Tanaka et al., 1995). Some properties and/or processes in physical systems are governed by conservation laws related to parity and total angular momentum of the system. Such systems are best described in terms of wave functions that have definite parity and angular momentum. The AMD wave function does not have definite parity nor does it possess definite total angular momentum. As a result, for applications in realistic investigations of properties of physical systems the AMD wave function requires some improvement. A number of modifications have since been introduced in the AMD formalism. In reference (Kanada-En'yo et al., 1995) numerical technique are used to project the AMD wave function onto the eigenstates of parity and total angular momentum. The resulting wave functions have definite parity and total angular momentum. In addition, a number of different techniques were considered for constructing a more flexible total wave function. One way was to use linear combinations

of variational spatial, spin and isospin functions to represent single-particle wave functions (Doté & Horiuchi, 2000; Doté et al., 2006). The resulting wave functions are suitable for investigating systems with tensor forces. The other approach is to use a linear combination of several Slater determinants (Kanada-En'yo et al., 1995; 2003; Kimura, 2004) to represent the total wave function of the system. In the approach of reference (Doté et al., 1997) orthogonal single-particle wave functions characteristic of the Hartree-Fock orbitals are constructed from the AMD wave function. The AMD+Hartree-Fock wave function is also more flexible than the original AMD wave function. These modifications to the AMD wave function introduced significant improvements in the description of ground-state properties, mean-field and cluster structure of nuclear systems. It should be noted that most of the studies indicated employed phenomenological nucleon-nucleon potentials of Gaussian radial form. The main reason for this is that the expectation values of this type of potentials can be evaluated analytically.

To extend the application of the AMD approach to realistic potentials further proposals were made. In Refs. (Togashi & Katō, 2007; Togashi et al., 2009) the *G*-matrix approach was used to incorporate two-body correlations in the wave function. The resulting Bruckner-AMD wave function can be constructed with realistic nuclear potentials. In Ref. (Watanabe et al., 2009; Watanabe & Oryu, 2006) Jacobi coordinates are employed to construct the wave function. Many-body correlations are included, more variational parameters are considered and the effects of the center-of-mass are completely and explicitly removed. Most realistic potentials are of non-Gaussian form and are, in many cases, expanded as the sum-of-Gaussian for application in the AMD approach. In Ref. (Rampho, 2011) a numerical technique of evaluating expectation values of non-Gaussian potentials is introduced. The technique approximates the expectation value of the potential operator with a rapidly converging series of Talmi integrals. This technique is further elaborated on in this work. Ground-state properties of selected few-nucleon systems are determined using the Argonne V4' nucleon-nucleon potential.

In section 2 the construction of the AMD wave function is outlined while the variational technique used to determine the variational parameters is briefly discussed in section 3. Application of AMD to selected light nuclei is presented in section 4 while section 5 is devoted to the charge form factors of ground state in three- and four-nucleon systems. Conclusions are given in section 6.

2. The AMD wave function

Consider a nuclear system consisting of A nucleons. The wave function Ψ describing the system depends on the position \vec{r}_i , spin $\vec{\sigma}_i$ and isospin $\vec{\tau}_i$ ($i = 1, 2, 3, \dots, A$), vectors of the nucleons. In what follows the collective vector, \vec{v}_i , is used to represent the set $\{\vec{s}_i \vec{r}_i \vec{\sigma}_i \vec{\tau}_i\}$ where \vec{s}_i is a complex variational parameter. For a systems of fermions, like nuclei, the total wave function is required to be antisymmetric with respect to the interchange of any two particles in the system. One way of constructing such a wave function is by the use of Slater determinants of single-particle wave functions $\psi_i(\vec{v}_j)$ as

$$\Psi_t(\vec{v}_1, \vec{v}_2, \vec{v}_3, \dots, \vec{v}_A) = \frac{1}{\sqrt{A!}} \begin{vmatrix} \psi_1(\vec{v}_1) & \psi_2(\vec{v}_1) & \psi_3(\vec{v}_1) & \cdots & \psi_A(\vec{v}_1) \\ \psi_1(\vec{v}_2) & \psi_2(\vec{v}_2) & \psi_3(\vec{v}_2) & \cdots & \psi_A(\vec{v}_2) \\ \psi_1(\vec{v}_3) & \psi_2(\vec{v}_3) & \psi_3(\vec{v}_3) & \cdots & \psi_A(\vec{v}_3) \\ \vdots & \vdots & \vdots & \ddots & \vdots \\ \psi_1(\vec{v}_A) & \psi_2(\vec{v}_A) & \psi_3(\vec{v}_A) & \cdots & \psi_A(\vec{v}_A) \end{vmatrix}. \quad (1)$$

The functions $\psi_i(\vec{v}_j)$ do not form an orthogonal basis. However, an orthonormal basis can be constructed from these functions (Doté et al., 1997; Togashi & Katō, 2007; Togashi et al., 2009). The ground state wave function of the system is represented by $\Psi_t(\vec{S})$ where $\vec{S} \equiv \{\vec{s}_1, \vec{s}_2, \vec{s}_3, \dots, \vec{s}_A\}$.

The single-particle wave function $\psi(\vec{v})$ is assumed to be separable in the form

$$\psi(\vec{v}) = \phi(\vec{s}, \vec{r}) \chi(\vec{\sigma}) \zeta(\vec{\tau}) \quad (2)$$

where $\phi(\vec{s}, \vec{r})$, $\chi(\vec{\sigma})$, and $\zeta(\vec{\tau})$ are the spatial, spin and isospin wave functions, respectively. The intrinsic spin state $\chi(\vec{\sigma})$ of a fermion, with spin s and third component of the spin m_s , is denoted by

$$\chi(\vec{\sigma}) = |s, m_s\rangle = \begin{cases} \left| \frac{1}{2}, +\frac{1}{2} \right\rangle = |\uparrow\rangle \\ \left| \frac{1}{2}, -\frac{1}{2} \right\rangle = |\downarrow\rangle \end{cases} \quad (3)$$

where $|\uparrow\rangle$ represents the *spin-up* and $|\downarrow\rangle$ the *spin-down* state. These two spin states are orthogonal to each other. To improve the quality of the wave function the spins of the fermions may be allowed to vary. This is done by representing the fermion spin as a general spinor. Such a spinor is expressed as a linear combination of the spin-up and spin-down states using complex variational parameters (Kanada-En'yo et al., 2003). The isospin state, $\zeta(\vec{\tau})$, in the case of a nucleon, with isospin t and third component of the isospin m_t , is given by

$$\zeta(\vec{\tau}) = |t, m_t\rangle = \begin{cases} \left| \frac{1}{2}, +\frac{1}{2} \right\rangle = |p\rangle \\ \left| \frac{1}{2}, -\frac{1}{2} \right\rangle = |n\rangle \end{cases} \quad (4)$$

where $|p\rangle$ refers to a proton while $|n\rangle$ refers to a neutron state. These states are time-independent also.

All the constituent particles are described by the same form of the spatial wave function. The spatial component, $\phi(\vec{s}, \vec{r})$, is parametrized as a normalized Gaussian wave packet (Ono et al., 1992)

$$\phi(\vec{s}, \vec{r}) = \left(\frac{2\alpha}{\pi} \right)^{3/4} \exp \left[-\alpha \left(\vec{r} - \frac{\vec{s}}{\sqrt{\alpha}} \right)^2 + \frac{\vec{s}^2}{2} \right]. \quad (5)$$

The phase $\vec{s}^2/2$ is included mainly to simplify the structure of the elements of the resulting overlap matrix, $\langle \phi_i | \phi_j \rangle$. The width parameter α is treated as a real constant and assumed to be the same for both protons and neutrons in the nucleus. It can be argued that the assumption is still valid if the masses of the constituents are not significantly different, like in nuclear systems. When the momentum operator of a fermion is denoted by \vec{p} , then the real component $\text{Re}[\vec{s}]$ and the imaginary component $\text{Im}[\vec{s}]$ of the parameter \vec{s} are given by

$$\text{Re}[\vec{s}] = \sqrt{\alpha} \frac{\langle \phi(\vec{r}) | \vec{r} | \phi(\vec{r}) \rangle}{\langle \phi(\vec{r}) | \phi(\vec{r}) \rangle} \quad \text{and} \quad \text{Im}[\vec{s}] = \frac{1}{2\hbar\sqrt{\alpha}} \frac{\langle \phi(\vec{r}) | \vec{p} | \phi(\vec{r}) \rangle}{\langle \phi(\vec{r}) | \phi(\vec{r}) \rangle}. \quad (6)$$

The single-particle wave function in Eq. (5) satisfies the minimum uncertainty $\Delta\vec{r}\Delta\vec{p} = \hbar/2$ (Ono & Horiuchi, 2004) which helps in the choice of the value for the width parameter α . Following Ref. (Ono et al., 1992), the value of α is chosen so as to generate reasonable description of the ground state properties of light nuclei. The expectation values of relevant operators calculated with this form of the wave function can be determined in analytical form.

A more realistic wave function is constructed from the AMD wave function (1) by projecting on to states with definite parity π and total angular momentum J . The parity projected wave function has the form

$$\Psi^\pi = \frac{1}{2} [1 \pm P^\pi] \Psi(\vec{S}) \quad (7)$$

where P^π is the parity projection operator. A wave function with a definite parity π , total angular momentum J , and angular momentum projections MK , is constructed from the AMD wave function as

$$\Psi_{MK}^{J\pi} = \frac{1}{2} P_{MK}^J(\Omega) [1 \pm P^\pi] \Psi_{AMD} \quad (8)$$

where $P_{MK}^J(\Omega)$ is the angular momentum projection operator, P^π the parity projection operator. The angular momentum projection operator is defined by (Peierls & Yoccoz, 1957)

$$P_{MK}^J(\Omega) = \frac{2J+1}{8\pi^2} \int d\Omega D_{MK}^{J*}(\Omega) \hat{R}(\Omega) \quad (9)$$

where $D_{MK}^J(\Omega)$ is the Wigner D -function and $\hat{R}(\Omega)$ the rotation operator with $\Omega \equiv \{\alpha, \beta, \gamma\}$ representing Euler rotation angles.

3. Equations of motion

The wave function of the system $\Psi(\vec{S})$ depends on the set of complex variational parameters \vec{S} . To establish the time evolution of such a wave function, the form of the time dependence of the variational parameters, and therefore the equations of motion, is determined. The equations of motion of the parameters are derived from the time-dependent variational principle (Kramer & Saraceno, 1981)

$$\delta \int_{t_1}^{t_2} \left[\frac{i\hbar}{2} \frac{\langle \Psi | \dot{\Psi} \rangle - \langle \dot{\Psi} | \Psi \rangle}{\langle \Psi | \Psi \rangle} - \frac{\langle \Psi | H | \Psi \rangle}{\langle \Psi | \Psi \rangle} \right] dt = 0 \quad (10)$$

with the constraints

$$\delta \Psi(t_1) = \delta \Psi(t_2) = \delta \Psi^*(t_1) = \delta \Psi^*(t_2) = 0 \quad (11)$$

where $\dot{\Psi} = d\Psi/dt$ and Ψ^* the complex conjugate of the wave function. In this definition of the variational principle the wave function Ψ is not normalized. Therefore the equations of motion for the variational parameters will not depend on either the normalization or the phase of the wave function. The variation of the wave function in Eq. (10) with respect to time can be cast in the form

$$\frac{d\Psi}{dt} = \sum_i \left[\frac{d\tilde{s}_i}{dt} \frac{\partial \Psi}{\partial \tilde{s}_i} + \frac{d\tilde{s}_i^*}{dt} \frac{\partial \Psi}{\partial \tilde{s}_i^*} \right]. \quad (12)$$

The equations of motion of the variational parameters can then be obtained by expressing Eq. (10) in terms of the parameters as

$$\delta \int_{t_1}^{t_2} \left[\frac{i\hbar}{2} \sum_j \left(\frac{d\tilde{s}_j}{dt} \frac{\partial}{\partial \tilde{s}_j} - \frac{d\tilde{s}_j^*}{dt} \frac{\partial}{\partial \tilde{s}_j^*} \right) \ln \langle \Psi | \Psi \rangle - E \right] dt = 0 \quad (13)$$

with the constraints

$$\delta \vec{s}(t_1) = \delta \vec{s}(t_2) = \delta \vec{s}^*(t_1) = \delta \vec{s}^*(t_2) = 0 \quad (14)$$

where

$$E(\vec{S}, \vec{S}^*) = \frac{\langle \Psi(\vec{S}) | H | \Psi(\vec{S}) \rangle}{\langle \Psi(\vec{S}) | \Psi(\vec{S}) \rangle} \quad (15)$$

is the energy functional of the system. Minimizing the action in Eq. (13) with the constraints (14) results in the equations

$$\frac{i\hbar}{2} \sum_i \left(\frac{\partial^2 \ln \langle \Psi | \Psi \rangle}{\partial \vec{s}_i \partial \vec{s}_j^*} \right) \frac{d\vec{s}_i}{dt} = \frac{\partial E}{\partial \vec{s}_j^*} \quad \text{and} \quad -\frac{i\hbar}{2} \sum_j \left(\frac{\partial^2 \ln \langle \Psi | \Psi \rangle}{\partial \vec{s}_i \partial \vec{s}_j^*} \right) \frac{d\vec{s}_j^*}{dt} = \frac{\partial E}{\partial \vec{s}_i} \quad (16)$$

of the variational parameters. Defining a Hermitian and positive definite matrix \mathcal{C} with elements

$$C_{ij} = \frac{\partial^2 \ln \langle \Psi | \Psi \rangle}{\partial \vec{s}_i \partial \vec{s}_j^*}, \quad (17)$$

the equations of motion can be compactly expressed in the form (Kramer & Saraceno, 1981)

$$\frac{i\hbar}{2} \begin{bmatrix} 0 & \mathcal{C} \\ -\mathcal{C}^* & 0 \end{bmatrix} \begin{bmatrix} \frac{d\vec{s}^*}{dt} \\ \frac{d\vec{s}}{dt} \end{bmatrix} = \begin{bmatrix} \frac{\partial E}{\partial \vec{s}^*} \\ \frac{\partial E}{\partial \vec{s}} \end{bmatrix}. \quad (18)$$

The solution to these equations provide the time evolution of the variational parameters and therefore of the wave function of the system.

To determine the parameters \vec{s}_i and the variational energy E of the system Eq. (18) are modified by multiplying the right-hand-side by a complex constant $\mu = a + ib$ where a and b are arbitrary real numbers. The coefficient μ introduce friction in the equations. The resulting equations can be solved numerically. To show that solving the modified equation of motion minimizes the energy the matrix \mathcal{C} is replaced by a simpler positive definite matrix, the unit matrix I (Ono & Horiuchi, 2004). Then the equations of motion for the variational parameters takes the form

$$\frac{d\vec{s}_i}{dt} = \frac{2\mu}{i\hbar} \frac{\partial E}{\partial \vec{s}_i^*} \quad \text{and} \quad \frac{d\vec{s}^*}{dt} = -\frac{2\mu^*}{i\hbar} \frac{\partial E}{\partial \vec{s}_i}. \quad (19)$$

These equations have a form similar to that of Hamilton's classical equations of motion for canonically conjugate variables. The variation of the energy functional with time leads to

$$\frac{dE}{dt} = \sum_i \left[\frac{\partial E}{\partial \vec{s}_i} \frac{d\vec{s}_i}{dt} + \frac{\partial E}{\partial \vec{s}_i^*} \frac{d\vec{s}_i^*}{dt} \right] = \frac{4b}{\hbar} \sum_i \frac{\partial E}{\partial \vec{s}_i} \frac{\partial E}{\partial \vec{s}_i^*}. \quad (20)$$

The same result can be obtained using the positive definite matrix \mathcal{C} (Ono & Horiuchi, 2004). Since the two terms in Eq. (20) are positive at all times, it is evident that

$$\frac{dE}{dt} < 0 \quad \text{when} \quad b < 0, \quad (21)$$

so that choosing $b < 0$ results in the energy functional decreasing with time during the variation of the parameters. Hence the parameter μ is referred to as the coefficient of friction and this technique of lowering the energy of a system is called *frictional cooling*. The equations

are solved with the constraint $\sum_i \vec{s}_i = 0$. The zero-point oscillation of the center-of-mass need be subtracted from the expectation value of the Hamiltonian of the system.

4. Nuclear ground state properties

To evaluate the variational energy functional and solve for the variation parameters, the Hamiltonian H of the nucleus is required as input. Considering only two-body interactions in the nucleus the nuclear Hamiltonian has the form

$$H = - \sum_i \frac{\hbar^2}{2m_i} \nabla_i^2 + \frac{1}{2} \sum_{i \neq j} [V_{NN}(\vec{r}_{ij}) + V_C(\vec{r}_{ij})] \quad (22)$$

where m_i is the mass of nucleon i , $V_{NN}(\vec{r})$ the nucleon-nucleon NN potential, $V_C(\vec{r})$ the Coulomb potential and \vec{r} the relative position vector of the interacting nucleons. In this work the AV4' NN potential with the $V_{C1}(\vec{r})$ Coulomb component is used (Wiringa & Pieper, 2002). In operator form the general Argonne nucleon-nucleon potential can be written in the form

$$V(\vec{r}_{ij}) = \sum_m v_m(r_{ij}) \mathcal{O}_{ij}^m \quad (23)$$

where $v_m(r_{ij})$ are radial form factors and \mathcal{O}_{ij}^m two-body nucleon operators. The Argonne V4' potential employed in this work consists of the first four operators

$$\mathcal{O}_{ij}^{1 \rightarrow 4} \equiv \{1, \vec{\sigma}_i \cdot \vec{\sigma}_j\} \otimes \{1, \vec{\tau}_i \cdot \vec{\tau}_j\}. \quad (24)$$

The V4 potential model can also be cast in the form

$$V(\vec{r}_{ij}) = \sum_{T=0}^1 \sum_{S=0}^1 V_{ST}^c(r_{ij}) \Omega_{ij}^{(S)} \Omega_{ij}^{(T)} \quad (25)$$

where the subscripts S (T) indicate the coupled spin (isospin) of the interacting nucleon pair. Using the transformations

$$\Omega_{ij}^{(S)} = \frac{1}{2} [1 + (-1)^{S+1} P_{ij}^\sigma] \quad \text{and} \quad \Omega_{ij}^{(T)} = \frac{1}{2} [1 + (-1)^{T+1} P_{ij}^\tau] \quad (26)$$

of the spin and isospin projection operators, respectively, where P_{ij}^σ (P_{ij}^τ) is the spin (isospin) exchange operator, one obtains

$$V(\vec{r}_{ij}) = V_c(r_{ij}) + V_\sigma(r_{ij}) P_{ij}^\tau - V_\tau(r_{ij}) P_{ij}^\sigma - V_{\sigma\tau}(r_{ij}) P_{ij}^\sigma P_{ij}^\tau. \quad (27)$$

The relation between the form factors in equations (23) and (27) are

$$V_c = v_c - v_\tau - v_\sigma + v_{\sigma\tau} \quad (28)$$

$$V_\tau = 2 [v_\tau - v_{\sigma\tau}] \quad (29)$$

$$V_\sigma = 2 [v_\sigma - v_{\sigma\tau}] \quad (30)$$

$$V_{\sigma\tau} = 4 v_{\sigma\tau} \quad (31)$$

where the dependence on r is understood. These radial form factors are very difficult to approximate satisfactorily with less than twenty Gaussian functions.

The variational energy E_0 , root-mean-square (rms) radius $\sqrt{\langle r^2 \rangle}$ and magnetic moment μ of the nuclei are calculated using the parity projected AMD wave function, Ψ^π . These three quantities are given by

$$E_0 = \frac{\langle \Psi^\pi | H | \Psi^\pi \rangle}{\langle \Psi^\pi | \Psi^\pi \rangle} \quad (32)$$

$$\langle r^2 \rangle = \frac{1}{A} \frac{\langle \Psi^\pi | \sum_{i=1}^A [\vec{r}_i - \vec{R}]^2 | \Psi^\pi \rangle}{\langle \Psi^\pi | \Psi^\pi \rangle} \quad (33)$$

$$\vec{\mu} = \frac{\langle \Psi^\pi | \sum_{i=1}^A [g_\ell \vec{\ell}_i + g_s \vec{s}_i] | \Psi^\pi \rangle}{\langle \Psi^\pi | \Psi^\pi \rangle} \quad (34)$$

where \vec{R} is the center-of-mass of the nucleus, $\vec{\ell}_i$ (\vec{s}_i) the orbital (spin) angular momentum and g_ℓ (g_s) the corresponding g -factor of a nucleon. The g -factors are constants with values (Wong, 1998)

$$g_\ell = \begin{cases} 1 & \text{for proton} \\ 0 & \text{for neutron} \end{cases} : \quad g_s = \begin{cases} 5.585695 & \text{for proton} \\ -3.826085 & \text{for neutron} \end{cases} \quad (35)$$

The integrals in equations (32), (33) and (34) can be analytically evaluated (Rampho, 2010). As an illustration the evaluation of the variational energy is summarized. The variational energy is evaluated as

$$E_0 = \sum_{ik} \mathcal{T}_{ik} B_{ik}^{-1} + \sum_{ijkl} \mathcal{V}_{ijkl} B_{li} B_{kj} [\mathcal{P}_{ij}^d B_{il}^{-1} B_{jk}^{-1} - \mathcal{P}_{ij}^e B_{ik}^{-1} B_{jl}^{-1}] \quad (36)$$

where the first sum generate the total kinetic energy while the second generate the total potential energy of the system. In this energy functional \mathcal{T}_{ik} and \mathcal{V}_{ijkl} represent the integrals involving the kinetic operator and potential functions, respectively, with $B_{ij} = \langle \psi_i | \psi_j \rangle$ and \mathcal{P}_{ij}^d (\mathcal{P}_{ij}^e) resulting from direct (exchange) interactions. The evaluation of the expectation values of the potential can be evaluated analytically when the these radial components are given in terms of Gaussian functions (Tohsaki, 1992). Instead of expanding the potential in terms of Gaussians the corresponding expectation value is approximated by the series (Rampho, 2011)

$$\mathcal{V}_{ijkl} = \exp\left(-\frac{\eta_2^2}{4}\right) \sum_{m=0}^{\infty} \left(\frac{\eta_2^2}{4}\right)^m I_\alpha(m) \quad (37)$$

where $\vec{\eta}_2 = \vec{s}_l - \vec{s}_k + \vec{s}_i - \vec{s}_j$ and

$$I_\alpha(m) = \frac{2\alpha^{m+3/2}}{\Gamma(m+1)\Gamma(m+\frac{3}{2})} \int_0^\infty r^{2m+2} V(r) e^{-\alpha r^2} dr \quad (38)$$

the Talmi integral involving the gamma function $\Gamma(x)$. If the range of the potential is not greater than $1/\sqrt{2\alpha}$ then the series in Eq. (37) converges quite fast for any value of $\vec{\eta}_2$ (Brink, 1965). Therefore, only the first few terms in the series tend to be significant. The Coulomb potential is treated with a Gaussian integral transform. In solving the cooling equations a random number generator is used to set up the initial values of the variational parameters. The required wave function is obtained when the energy functional for the system is independent of the variations of the parameters of the wave function. The parity projection of the wave functions is done before the variation of the parameters. Only the first five terms

of the series in (37) were considered. The integral in $I_\alpha(m)$ is evaluated numerically using a Gaussian quadrature. The value of α was chosen to satisfactorily reproduce the experimental binding energy of the three-nucleon systems. The variational energies are corrected by subtracting contributions from spurious center-of-mass. The results are presented along with corresponding experimental data in Table 1. As can be observed from this table the theoretical prediction of the experimental binding energies of the three-nucleon systems is satisfactory, as expected. However, the experimental binding energy of the ^2H nucleus is overestimated by about 60 %. The binding energy of the ^4He nucleus is underestimated by 10 % whereas that of the ^6Li and ^8Be nuclei are underestimated by 14 %. The ^8Be nucleus is very unstable (Audi et al., 2003) and, therefore, very challenging to study experimentally.

The AMD generates reasonable predictions of the experimental values for the rms radii of the nuclei. The deviation of the predicted values from the experimental values for the nuclei range from 0 %, for the ^3He nucleus, to 11 %, for the ^6Li nucleus. The theoretical radii of the ^6Li and the ^8Be nuclei are almost the same. In general the theoretical results overestimate the experimental values of the rms radii for all the nuclei. The calculated magnetic moments of the three-nucleon systems are different from the experimental values by 6 % and 10 %. For the three-nucleon systems the theoretical moments equal the magnetic moment of the unlike nucleon in the system. This reason also explains why the calculated magnetic moments of the ^2H and ^6Li nuclei, which overestimate the respective experimental values by 3 % and 7 %, are equal. The calculated magnetic moments of the ^4He and ^8Be nuclei are both equal to zero. These results are consistent with the theoretical expectation when only the dominant spherical ground state wave function of the system is used in the calculations (Phillips, 1977). The results for the parity and angular momentum projected wave function are given in Table 2 for the three-nucleon and the four-nucleon systems. The parity projection is done before the variation of the parameters and the angular momentum projection is done after the optimisation of the parameters. The rotation increases the theoretical energies of the three-nucleon systems by 10 % and decreases that of the four-nucleon system by 10 %, relative to the un-rotated wave function. Since the nuclear systems are described with spherical wave functions, spatial rotations are not expected to introduce significant modifications to the results presented in Table 1. The binding energy found for the ^3H system overestimates

$^A\chi^\pi$	E_0 (MeV)		$\sqrt{\langle r^2 \rangle}$ (fm)		μ (μ_N)	
	AMD	EXP	AMD	EXP	AMD	EXP
$^2\text{H}^+$	-3.53	-2.23	2.16	1.96	0.880	0.857
$^3\text{H}^+$	-8.12	-8.48	1.76	1.60	2.793	2.979
$^3\text{He}^+$	-7.78	-7.72	1.76	1.77	-1.913	-2.128
$^4\text{He}^+$	-25.50	-28.3	1.53	1.47	0.000	
$^6\text{Li}^+$	-27.54	-31.99	2.70	2.4	0.880	0.822
$^8\text{Be}^+$	-49.38	-55.99	2.75		0.000	

Table 1. The ground state energies, rms radii and magnetic moments of selected light nuclei. The experimental data are taken from reference (Suzuki et al., 2008).

$^A\chi(J^\pi)$	E_0 (MeV)		$\sqrt{\langle r^2 \rangle}$ (fm)		μ (μ_N)	
	AMD	EXP	AMD	EXP	AMD	EXP
$^3\text{H}(\frac{1}{2}^+)$	-8.95	-8.48	1.33	1.60	2.769	2.979
$^3\text{He}(\frac{1}{2}^+)$	-8.61	-7.72	1.33	1.77	-1.847	-2.128
$^4\text{He}(0^+)$	-23.04	-28.30	1.16	1.47	0.000	

Table 2. The ground state energies, rms radii and magnetic moments of the three- and four-nucleon systems. The experimental values are taken from reference (Suzuki et al., 2008).

the experimental energy by 5 % and for the ^3He system by 12 %. In contrast, the ^4He results are lower than the experimental value by $\sim 19 \%$, a result which is in line with other calculations in the field using the same rank in the potential. The rms radii obtained for the ^3H and ^3He systems are lower than the experimental values by $\sim 16 \%$ and $\sim 22 \%$ less, respectively. Similar results are obtained for the ^4He system where the calculated rms radius is underestimated by $\sim 21 \%$. In general, the AMD approach reproduces the experimental values for the magnetic moment of the nuclei quite satisfactorily.

Intrinsic density distribution in a nucleus is determined by rotating the arbitrary space-fixed coordinate axes on to the body-fixed principal axes of the nucleus. The rotation is generated by diagonalising the moment-of-inertia tensor of the nucleus which is defined by elements

$$I_{\mu\nu} = \frac{\langle \Psi^\pi | \sum_{i=1}^A [\vec{r}_i - \vec{R}]_\mu [\vec{r}_i - \vec{R}]_\nu | \Psi^\pi \rangle}{\langle \Psi^\pi | \Psi^\pi \rangle}$$

(39)

where $\{\mu, \nu\} \equiv \{x, y, z\}$. The calculated intrinsic density using the parity projected wave function, in the body-fixed coordinate axes, are shown in Figure 1 for the ^4He nucleus and in Figure 2 for the ^6Li and ^8Be nuclei. The ^4He nuclei displays a spherical density distribution whereas the ^6Li and ^8Be nuclei display distinct cluster structures.

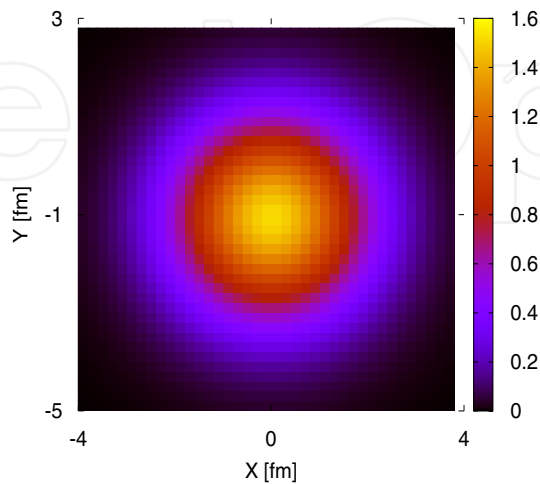


Fig. 1. Density distribution of the ^4He nucleus.

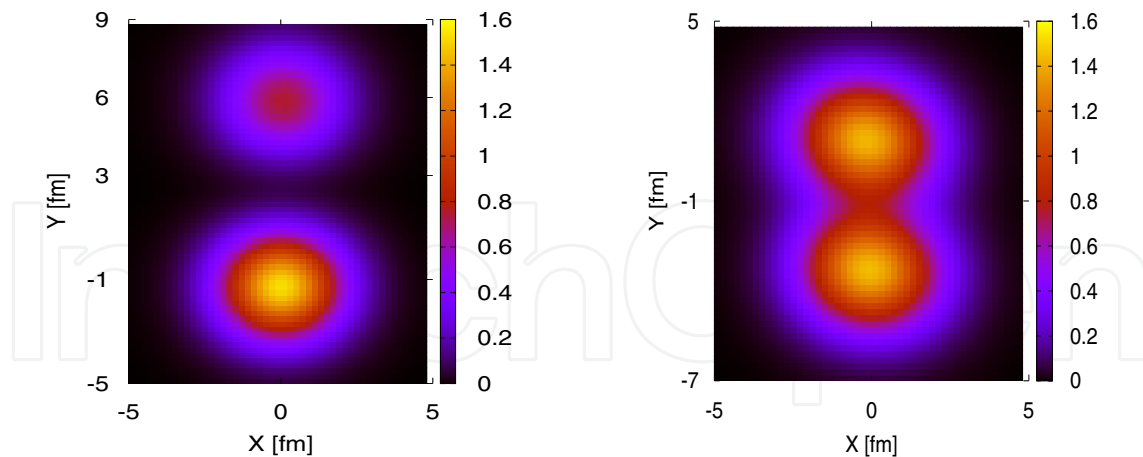


Fig. 2. Density distributions of the ${}^6\text{Li}$ nucleus (left) and the ${}^8\text{Be}$ nucleus (right).

5. Charge form factors

Most of the information accumulated about nuclear structure is derived from electron-nucleus scattering. In electron-nucleus scattering the electron transfers momentum \vec{q} and energy ω to the target nucleus and the nucleus undergoes some transitions that are governed by selection rules related angular momentum and parity. For elastic scattering the initial and final states of the nucleus have the same angular momentum (de Forest Jr. & Walecka, 1966). This type of electron scattering is used to probe ground state charge and magnetisation distributions in nuclei. The ground state of the ${}^3\text{He}$ nucleus has total angular momentum and parity $J^\pi = \frac{1}{2}^+$ whereas the ${}^4\text{He}$ system has $J^\pi = 0^+$. Theoretical predictions of electromagnetic provide a good test of the quality of the wave function describing the system. In this section the charge form factors of ${}^3\text{He}$ and ${}^4\text{He}$ nuclei are calculated in the plane wave impulse approximation (PWIA) (Chew & Wick, 1952). In this approximation the nucleons inside the target nucleus are assumed non-interacting with one another during the interaction with the electron. This means that the electron interacts with independent nucleons inside the nucleus. Since the transitions are between states of definite angular momentum, the parity and angular momentum projected wave functions are employed.

The charge distribution in the nucleus is inferred from the electric transitions in the nucleus due elastic electron-nucleus scattering. The charge form factor is the expectation value of the nuclear charge operator. For a nucleus in an initial state $|\Psi_{MK}^{J\pi}\rangle$ the charge form factor is given by

$$F_{\text{ch}}(\vec{q}) = \frac{1}{Z} \frac{\langle \Psi_{MK}^{J\pi} | \rho(\vec{q}) | \Psi_{MK}^{J\pi} \rangle}{\langle \Psi_{MK}^{J\pi} | \Psi_{MK}^{J\pi} \rangle} \quad (40)$$

where Ze is the total charge on and $\rho(\vec{q})$ the charge operator of the nucleus with \vec{q} being the momentum transferred to the nucleus by the electron. In the PWIA the nuclear charge operator is formed by the superposition of the individual nucleon charge operators and is given by (Rampho, 2010)

$$\rho(\vec{q}) = \sum_{k=1}^A \left[\frac{q}{Q} G_{Ek}^N(Q^2) - \frac{2 G_{Mk}^N(Q^2) - G_{Ek}^N(Q^2)}{4 m_N^2 \sqrt{1 + \tau}} i \vec{\sigma}_k \cdot \vec{q} \times \vec{p}_k \right] \exp(i \vec{q} \cdot \vec{r}_k) \quad (41)$$

where $\tau = Q^2/4m_N^2$, $Q^2 = q^2 - \omega^2$, $\omega = \sqrt{q^2 + m_N^2} - m_N$ and G_E^N (G_M^N) the nucleon Sachs electric (magnetic) form factor. For the Sachs form factors the phenomenological parametrization derived in Ref. (Friedrich & Walcher, 2003) is adopted. The general multipole analysis of nuclear charge form factors is given by (Uberall, 1971)

$$F_{\text{ch}}(\vec{q}) = \sqrt{4\pi} \sum_{L=0}^{\leq 2J} \langle JJL0|JJ \rangle F_L^0(q) Y_{L0}^*(\hat{\mathbf{q}}) \quad (42)$$

where $Y_{LM}^*(\hat{\mathbf{q}})$ are the spherical harmonics, L the nuclear orbital angular momentum and $\langle JJL0|JJ \rangle$ the Clebsch-Gordan coefficients and $\hat{\mathbf{q}} = \vec{q}/|\vec{q}|$. The summation is over even values of L only. The intrinsic charge form factor is corrected by dividing the calculated charge form factor by the contributions of the center-of-mass (Rapho, 2010). The integrals in Eq. (42) can be analytically evaluated.

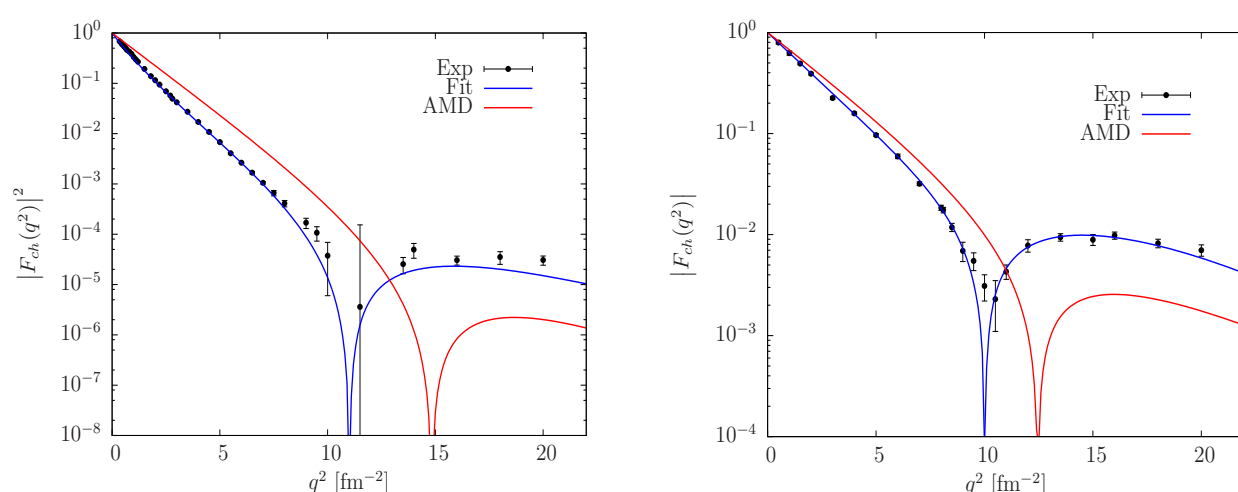


Fig. 3. The charge form factor of ^3He (left) and ^4He (right) compared with the experimental data of (McCarthy et al., 1977) and the theoretical fit to the data (Amroun et al., 1994).

The results of the calculated ground-state charge form factors of the ^3He and ^4He nuclei are presented in Figure 3. In these figures the theoretical charge form factors are compared with experimental data from (Frosch et al., 1967; McCarthy et al., 1977). In the comparison phenomenological parametrization (Amroun et al., 1994) that fit experimental universal data of the form factors for electron-nucleus scattering are also shown. The charge form factors are normalized such that $F_{\text{ch}}(0) = 1$. As can be seen in these figures, for low momentum transfers, up to the first diffraction minimum, the AMD gives a reasonable description, albeit it slightly overestimates the experimental data. Beyond the first diffraction minimum the results are lower than the data. The first diffraction minimum for the nuclei are consistent with, but not better than, the predictions of other theoretical models obtained with various nucleon-nucleon potentials in the PWIA (Kloet & Tjon, 1974). It should be noted that the overestimation of the position of the diffraction minimum indicates an underestimation of the nuclear charge radius.

6. Conclusions

To test the applicability of the AMD model in nuclear structure studies, the angular momentum and parity projected AMD wave function were used to calculate binding energies,

rms radii, and the magnetic moments for selected few-nucleon systems. The nuclear Hamiltonian was constructed from the Argonne AV4' NN potential that includes also the Coulomb interaction. Comparison with the experimental data revealed that the reproduction of the ground state properties of light nuclei is quite satisfactory. The discrepancies observed can be attributed to reasons not entirely related to the AMD. These include i) the omission of mixed-symmetric states (for three-body) ii) the use of a limited rank for the Argonne AV18 potential, and iii) the omission of three-nucleon forces. As far as the magnetic moment is concerned, the inclusion of relativistic corrections to the magnetic moment operator, are also expected to contribute to the reduction of the discrepancy between theory and experiment. The technique used in the approximation of the variational energy can be easily extended to the three-body interactions. The implementation of this technique in nuclear three-body interactions will be considered future projects.

The angular momentum and parity projected AMD was used to calculate the ground state charge form factors for the ^3He and ^4He nuclei. In overall, the results obtained, within the AMD and PWIA approximation, reproduce the general behavior of the experimental form factors. For momentum transfer below the first diffraction minimum the reproduction of experimental form factors is fairly good. However, beyond the first diffraction minimum the results are lower than the data. The deviations of the theoretical results from experimental data can be minimize by employing improved wave functions. The wave functions can be constructed by using a more complete realistic Hamiltonian, three-body forces, and relativistic corrections in the electromagnetic operators. It should be noted that these results are consistent with other results obtained by competing theoretical models. In conclusion, the results indicate that the AMD method is a very promising method in calculating electromagnetic form factors of the general A -body nuclear system.

Work is underway to construct wave functions for scattering processes applicable in nuclear breakup reactions (Rampho, 2010). In these constructs the AMD is combined with the Glauber multiple scattering to account for final state interactions. Wave functions for two-body and three-body scattering reactions can be treated accurately in the Faddeev formalism (Golak et al., 2005; Merkuriev et al., 1976). In the hyperspherical harmonics approach some progress in being made towards the construction of accurate wave functions for two-body scattering processes (Kievsky et al., 2008). However, these methods become involved for systems consisting of more than four constituent particles.

7. References

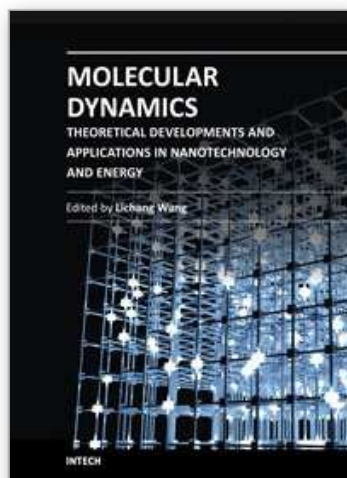
- Aichelin, J. (1991). "Quantum" molecular dynamics - a dynamical microscopic n -body approach to investigate fragment formation and the nuclear equation of state in heavy ion collisions, *Phys. Rep.* 202(5): 233–360.
- Alvioli, M., Ciofi degli Atti, C. & Morita, H. (2008). Proton-neutron and proton-proton correlations in medium-weight nuclei and the role of the tensor force, *Phys. Rev. Lett.* 100(16): 162503.
- Amroun, A., Breton, V., Cavedon, J. M., Frois, B., Goutte, D., Juster, F. P., Leconte, P., Martino, J., Mizuno, Y., Phan, X. H., Platchkov, S. K., Sick, I. & Williamson, S. (1994). ^3H and ^3He electromagnetic form factors, *Nucl. Phys. A* 579(3-4): 596–626.
- Audi, G., Bersillon, O., Blachot, J. & Wapstra, A. (2003). The NUBASE evaluation of nuclear and decay properties, *Nucl. Phys. A* 729(1): 3–128.

- Boffi, S., Bouten, M., Ciofi degli Atti, C. & Sawicki, J. (1968). Elastic and quasi-free electron scattering from ^{12}C and projected hartree-fock wave functions, *Nucl. Phys. A* 120(1): 135–144.
- Brink, D. (1965). The alpha-particle model of light nuclei, in C. Bloch (ed.), *Proceedings of the International School of Physics "Enrico Fermi"*, Vol. 36, Academic Press, New York, pp. 247–276.
- Carlson, J. & Schiavilla, R. (1998). Structure and dynamics of few-nucleon systems, *Rev. Mod. Phys* 70(3): 743–841.
- Caurier, E., Grammaticos, B. & Sami, T. (1982). The time dependent cluster model, *Phys. Lett. B* 109(3): 150–154.
- Chew, G. F. & Wick, G. C. (1952). The impulse approximation, *Phys. Rev.* 85(4): 636–642.
- Cottingham, W. N., Lacombe, M., Loiseau, B., Richard, J. M. & Mau, R. V. (1973). Nucleon-nucleon interaction from pion-nucleon phase-shift analysis, *Phys. Rev. D* 8(3): 800–819.
- de Forest Jr., T. & Walecka, J. D. (1966). Electron scattering and nuclear structure, *Adv. Phys.* 15(57): 1–109.
- Donnelly, T. W. & Raskin, A. S. (1986). Considerations of polarization in inclusive electron scattering from nuclei, *Ann. Phys.* 169(2): 247–351.
- Doté, A. & Horiuchi, H. (2000). Study of he isotopes with amd+hartree-fock, *Prog. Theor. Phys.* 103(2): 261–283.
- Doté, A., Horiuchi, H. & Kanada-En'yo, Y. (1997). Antisymmetrized molecular dynamics plus hartree-fock model and its application to be isotopes, *Phys. Rev. C* 56(4): 1844–1854.
- Doté, A., Kanada-En'yo, Y., Horiuchi, H., Akaishi, Y. & Ikeda, K. (2006). Explicit treatment of the tensor force with the method of antisymmetrized molecular dynamics, *Prog. Theor. Phys.* 115(6): 1069–1092.
- Egiyan, K. S., Asryan, G., Gevorgyan, N., Griffioen, K. A. & et al. (2007). Experimental study of exclusive $^2\text{H}(e, e'p)n$ reaction mechanisms at high Q^2 , *Phys. Rev. Lett.* 98(26): 262502.
- Egiyan, K. S., Dashyan, N. B., Sargsian, M. M., Strikman, M. I. & et al. (2006). Measurement of two- and three-nucleon short-range correlation probabilities in nuclei, *Phys. Rev. Lett.* 96(8): 082501.
- Engel, A., Tanaka, E. I., Maruyama, T., Ono, A. & Horiuchi, H. (1995). Δ degrees of freedom in antisymmetrized molecular dynamics and (p, p') reactions in the Δ region, *Phys. Rev. C* 52(6): 3231–3248.
- Feldmeier, H. (1990). Fermionic molecular dynamics, *Nucl. Phys. A* 515(1): 147–172.
- Frankfurt, L. L., Strikman, M. I., Day, D. B. & Sargsian, M. (1993). Evidence for short-range correlations from high q^2 (e, e') reactions, *Phys. Rev. C* 48(5): 2451–2461.
- Friedrich, J. & Walcher, T. (2003). A coherent interpretation of the form factors of the nucleon in terms of a pion cloud and constituent quarks, *Eur. Phys. J. A* 17(4): 607–623.
- Frosch, R. F., McCarthy, J. S., Rand, R. E. & Yearian, M. R. (1967). Structure of the ^4He nucleus from elastic electron scattering, *Phys. Rev.* 160(4): 874–879.
- Golak, J., Skibiński, R., Witala, H., Glöckle, W., Nogga, A. & Kamada, H. (2005). Electron and photon scattering on three-nucleon bound states, *Phys. Rep.* 415(2): 89–205.
- Horiuchi, H. (1991). Microscopic study of clustering phenomena in nucle, *Nucl. Phys. A* 522(1): 257–274.
- Jones, M. K., Aniol, K. A., Baker, F. T., Berthot, J. & et al. (2000). G_{E_p}/G_{M_p} ratio by polarization transfer in $\vec{e}p \rightarrow e\vec{p}$, *Phys. Rev. Lett.* 84(7): 1398–1402.
- Kamada, H., Nogga, A., Glöckle, W., Hiyama, E., Kamimura, M., Varga, K., Suzuki, Y., Viviani, M., Kievsky, A., Rosati, S., Carlson, J., Pieper, S. C., Wiringa, R. B., Navrátil, P., Barrett,

- B. R., Barnea, N., Leidemann, W. & Orlandini, G. (2001). Benchmark test calculation of a four-nucleon bound state, *Phys. Rev. C* 64(4): 044001.
- Kanada-En'yo, Y., Horiuchi, H. & Ono, A. (1995). Structure of li and be isotopes studied with antisymmetrized molecular dynamics, *Phys. Rev. C* 52(2): 628–646.
- Kanada-En'yo, Y., Kimura, M. & Horiuchi, H. (2003). Antisymmetrized molecular dynamics: a new insight into the structure of nuclei, *C. R. Physique* 4(4): 497–520.
- Kievsky, A., Rosati, S., Viviani, M., Marcucci, L. E. & Girlanda, L. (2008). A high-precision variational approach to three- and four-nucleon bound and zero-energy scattering states, *J. Phys. G: Nucl. Part. Phys.* 35(6): 063101.
- Kimura, M. (2004). Deformed-basis antisymmetrized molecular dynamics and its application to ^{20}Ne , *Phys. Rev. C* 69(4): 044319.
- Kloet, W. M. & Tjon, J. A. (1974). Meson exchange effects on the charge form factors of the tri-nucleon system, *Phys. Lett. B* 49(5): 419–422.
- Kramer, P. & Saraceno, M. (1981). *Geometry of the Time-Dependent Variational Principle in Quantum Mechanics*, Vol. 140, Springer-Verlag, Berlin, Germany.
- Lagaris, I. E. & Pandharipande, V. R. (1981). Phenomenological two-nucleon interaction operator, *Nucl. Phys. A* 359(2): 331–348.
- Machleidt, R., Holinde, K. & Elster, C. (1987). The bonn meson-exchange model for the nucleon-nucleon interaction, *Phys. Rep.* 149: 1–89.
- McCarthy, J. S., Sick, I. & Whitney, R. R. (1977). Electromagnetic structure of the helium isotopes, *Phys. Rev. C* 15(4): 1396–1414.
- Merkuriev, S. P., Gignoux, C. & Laverne, A. (1976). Three-body scattering in configuration space, *Ann. Phys.* 99(1): 30–71.
- Nagels, M. M., Rijken, T. A. & de Swart, J. J. (1978). Low-energy nucleon-nucleon potential from regge-pole theory, *Phys. Rev. D* 17(3): 768–776.
- Neff, T., Feldmeier, H. & Roth, R. (2005). Structure of light nuclei in fermionic molecular dynamics, *Nucl. Phys. A* 752: 321–324.
- Ono, A. & Horiuchi, H. (2004). Antisymmetrized molecular dynamics for heavy ion collisions, *Prog. Part. Nucl. Phys.* 53(2): 501–581.
- Ono, A., Horiuchi, H., Maruyama, T. & Ohnishi, A. (1992). Antisymmetrized version of molecular dynamics with two-nucleon collisions and its application to heavy ion reactions, *Prog. Theor. Phys.* 87(5): 1185–1206.
- Peierls, R. E. & Yoccoz, J. (1957). The collective model of nuclear motion, *Proc. Phys. Soc. A* 70(5): 381–387.
- Phillips, A. C. (1977). Three-body systems in nuclear physics, *Rep. Prog. Phys.* 40(8): 905–961.
- Piasetzky, E., Sargsian, M., Frankfurt, L., Strikman, M. & Watson, J. W. (2006). Evidence for strong dominance of proton-neutron correlations in nuclei, *Phys. Rev. Lett.* 97(16): 162504.
- Rampho, G. J. (2010). *Electromagnetic Processes in Few-Body Systems*, PhD thesis, Physics, University of South Africa.
- Rampho, G. J. (2011). Antisymmetrised molecular dynamics with realistic nucleon-nucleon potentials, *Few-Body Syst.* 50(1): 467–469.
- Schroeder, L. S., Chessin, S. A., Geaga, J. V., Grossiord, J. Y., Harris, J. W., Hendrie, D. L., Treuhaft, R. & Bibber, K. V. (1979). Energy dependence of charged pions produced at 180° in 0.8–4.89-gev proton-nucleus collisions, *Phys. Rev. Lett.* 43(24): 1787–1791.
- Suzuki, Y., Horiuchi, W., Orabi, M. & Arai, K. (2008). Global-vector representation of the angular motion of few-particle systems II, *Few-Body Syst.* 42(1): 33–72.

- Tanaka, E. I., Ono, A., Horiuchi, H., Maruyama, T. & Engel, A. (1995). Proton inelastic scattering to continuum studied with antisymmetrized molecular dynamics, *Phys. Rev. C* 52(1): 316–325.
- Togashi, T. & Katō, K. (2007). Brueckner-amd method and its applications to light nuclei, *Prog. Theor. Phys.* 117(1): 189–194.
- Togashi, T., Murakami, T. & Katō, K. (2009). Description of nuclear structures with brueckner-amd plus J^π projection, *Prog. Theor. Phys.* 121(2): 299–317.
- Tohsaki, A. (1992). Microscopic representation of α -cluster matter. I, *Prog. Theor. Phys.* 88(6): 1119–1129.
- Uberall, H. (1971). *Electron Scattering from Complex Nuclei: Part A*, Academic Press, New York.
- Ulmer, P. E., Aniol, K. A., Arenhövel, H. & et al. (2002). $^2\text{H}(e, e'p)n$ reaction at high recoil momenta, *Phys. Rev. Lett.* 89(6): 062301.
- Watanabe, T., Oosawa, M., Saito, K. & Oryu, S. (2009). A new molecular dynamics calculation and its application to the spectra of light and strange baryons, *J. Phys. G: Nucl. Part. Phys.* 36(1): 015001.
- Watanabe, T. & Oryu, S. (2006). A new antisymmetrized molecular dynamics approach to few-nucleon systems, *Prog. Theor. Phys.* 116(2): 429–434.
- Wiringa, R. B. & Pieper, S. C. (2002). Evolution of nuclear spectra with nuclear forces, *Phys. Rev. Lett.* 89(18): 182501.
- Wiringa, R. B., Smith, R. A. & Ainsworth, T. L. (1984). Nucleon-nucleon potentials with and without $\Delta(1232)$ degrees of freedom, *Phys. Rev. C* 29(4): 1207–1221.
- Wong, S. S. M. (1998). *Introductory Nuclear Physics*, 2 edn, John Wiley and Sons Inc., New York.

IntechOpen



Molecular Dynamics - Theoretical Developments and Applications in Nanotechnology and Energy

Edited by Prof. Lichang Wang

ISBN 978-953-51-0443-8

Hard cover, 424 pages

Publisher InTech

Published online 05, April, 2012

Published in print edition April, 2012

Molecular Dynamics is a two-volume compendium of the ever-growing applications of molecular dynamics simulations to solve a wider range of scientific and engineering challenges. The contents illustrate the rapid progress on molecular dynamics simulations in many fields of science and technology, such as nanotechnology, energy research, and biology, due to the advances of new dynamics theories and the extraordinary power of today's computers. This first book begins with a general description of underlying theories of molecular dynamics simulations and provides extensive coverage of molecular dynamics simulations in nanotechnology and energy. Coverage of this book includes: Recent advances of molecular dynamics theory Formation and evolution of nanoparticles of up to 106 atoms Diffusion and dissociation of gas and liquid molecules on silicon, metal, or metal organic frameworks Conductivity of ionic species in solid oxides Ion solvation in liquid mixtures Nuclear structures

How to reference

In order to correctly reference this scholarly work, feel free to copy and paste the following:

Gaotsiwe J. Rampho and Sofianos A. Sofianos (2012). Antisymmetrized Molecular Dynamics and Nuclear Structure, Molecular Dynamics - Theoretical Developments and Applications in Nanotechnology and Energy, Prof. Lichang Wang (Ed.), ISBN: 978-953-51-0443-8, InTech, Available from:
<http://www.intechopen.com/books/molecular-dynamics-theoretical-developments-and-applications-in-nanotechnology-and-energy/antisymmetrized-molecular-dynamics-and-nuclear-structure>

INTech
open science | open minds

InTech Europe

University Campus STeP Ri
Slavka Krautzeka 83/A
51000 Rijeka, Croatia
Phone: +385 (51) 770 447
Fax: +385 (51) 686 166
www.intechopen.com

InTech China

Unit 405, Office Block, Hotel Equatorial Shanghai
No.65, Yan An Road (West), Shanghai, 200040, China
中国上海市延安西路65号上海国际贵都大饭店办公楼405单元
Phone: +86-21-62489820
Fax: +86-21-62489821

© 2012 The Author(s). Licensee IntechOpen. This is an open access article distributed under the terms of the [Creative Commons Attribution 3.0 License](https://creativecommons.org/licenses/by/3.0/), which permits unrestricted use, distribution, and reproduction in any medium, provided the original work is properly cited.

IntechOpen

IntechOpen